



Li, Ke and Evans, Paul and Johnson, Mark (2017)
SiC/GaN power semiconductor devices: a theoretical
comparison and experimental evaluation under different
switching conditions. IET Electrical Systems in
Transportation . ISSN 2042-9738 (In Press)

Access from the University of Nottingham repository:

http://eprints.nottingham.ac.uk/44689/1/Final_version%20%28002%29%20Li.pdf

Copyright and reuse:

The Nottingham ePrints service makes this work by researchers of the University of Nottingham available open access under the following conditions.

This article is made available under the University of Nottingham End User licence and may be reused according to the conditions of the licence. For more details see:
http://eprints.nottingham.ac.uk/end_user_agreement.pdf

A note on versions:

The version presented here may differ from the published version or from the version of record. If you wish to cite this item you are advised to consult the publisher's version. Please see the repository url above for details on accessing the published version and note that access may require a subscription.

For more information, please contact eprints@nottingham.ac.uk

SiC/GaN Power Semiconductor Devices: A Theoretical Comparison and Experimental Evaluation under Different Switching Conditions

Ke Li^{1,*}, Paul Evans¹, Mark Johnson¹

¹Power Electronics, Machine and Control group, University of Nottingham, UK

*ke.li@nottingham.ac.uk

Abstract: (The paper is for special section “Design, modeling and control of electric drives for transportation applications”) The conduction and switching losses of SiC and GaN power transistors are compared in this paper. Voltage rating of commercial GaN power transistors is less than 650V while that of SiC power transistors is less than 1200V. The paper begins with a theoretical analysis that examines how the characteristics of a 1200V SiC-MOSFET change if device design is re-optimised for 600V blocking voltage. Afterwards, a range of commercial devices (1200V SiC-JFET, 1200V SiC-MOSFET, 650V SiC-MOSFET and 650V GaN-HEMT) with the same current rating are characterised experimentally and their conduction losses, inter-electrode capacitances and switching energy E_{sw} are compared, where it is shown that GaN-HEMT has smaller ON-state resistance, inter-electrode capacitance values and E_{sw} than SiC devices. Finally, in order to reduce device E_{sw} , a zero voltage switching circuit is used to evaluate all the devices, where device only produces turn-OFF switching losses and it is shown that GaN-HEMT has less switching losses than SiC device in this soft switching mode. It is also shown in the paper that 1200V SiC-MOSFET has smaller conduction and switching losses than 650V SiC-MOSFET.

1. Introduction

Electrical vehicle (EV) is an essential technology in the global fight to reduce environmental pollution and harmful gas emissions [1]. Power electronics systems are important for electrical energy conversion within EVs [2], where power semiconductor devices play an important role. Understanding power semiconductor devices characteristics is crucial for engineers to design high efficiency, high power density power converters so as to improve overall performance of electrical vehicles such as increase range and reliability.

Wide bandgap power semiconductor devices such as silicon carbide (SiC) and gallium nitride (GaN) have recently become a hot research topic because they are able to operate in higher temperature, higher frequency and realize higher energy conversion efficiency in comparison with traditional silicon (Si) power semiconductor devices. Commercial SiC transistors (JFET, MOSFET) can block voltage above 1200V and GaN transistor (HEMT) is able to withstand a maximal voltage of 650V, while they can conduct current from a few amperes to a few tens of amperes. Both SiC and GaN devices can be applied in electrical vehicles, in which the voltage rating of different electrical systems is found to be from low voltage to high voltage. Low voltage is normally from 12V to 42V and mainly for vehicle electrical equipment, where GaN devices can be used; while high voltage can reach up to 600V and is mainly for vehicle motor drive, where SiC devices can be used because of their high voltage rating. The voltage rating of battery pack in an EV can vary

from 200V to 400V, and it is found in the literature that both SiC and GaN devices are applied in vehicle based battery charger [3, 4].

When power semiconductor devices convert energy, they produce losses. Knowing SiC and GaN power devices losses is helpful in order to choose appropriate devices for vehicle-based power electronics systems. It is reported in the literature the experimental comparisons between SiC and Si power semiconductor devices [5] or between GaN and Si power semiconductor devices [6]. However, few publications are focused on experimental comparison between SiC and GaN power semiconductor devices due to their voltage rating mismatch.

Previous study on device losses comparison have been reported by authors in [7, 8]. The objective of this paper is to theoretically analyze SiC devices losses change when blocking voltage reduces from 1200V to 600V and then experimentally evaluate commercial SiC and GaN devices switching losses in different switching conditions. Using soft switching technique such as zero voltage switching (ZVS) helps to reduce device switching losses, so all the devices are also compared under soft-switching condition, which presents more experimental results than previous work in [7, 8].

The paper is structured with following sections: at first, SiC power devices conduction loss and switching loss change when reducing device blocking voltage is theoretically analyzed. Afterwards, different commercial SiC and GaN power devices ON-state resistance and inter-electrode capacitances values are compared. Then, those devices switching energy under hard and soft switching conditions are compared and conclusions are given finally.

2. Theoretical comparison

2.1. Conduction loss comparison

As shown in Fig. 1(a), ON-state resistance R_{ON} of a MOSFET is mainly composed by device channel resistance R_{ch} and drift region resistance R_{drift} .

This relationship can be expressed in terms of specific resistance ($m\Omega \cdot mm^2$) obtained by multiplying resistance by device active area in the following equation:

$$R_{ON,sp} = R_{ch,sp} + R_{drift,sp} \quad (1)$$

Demonstrated in [9], device minimal $R_{drift,sp}$ is proportional to device maximal blocking voltage $V_{DSS}^{2.5}$. Meanwhile, device $R_{drift,sp}$ is also proportional to device drift region thickness W_D . Thus, device $R_{drift,sp}$ and W_D value of a 600V and a 1200V device follow the same relation, which is given in eq.(2).

$$\frac{R_{drift,sp,600V}}{R_{drift,sp,1200V}} = \frac{W_{D,600V}}{W_{D,1200V}} \approx \frac{1}{5.6} \quad (2)$$

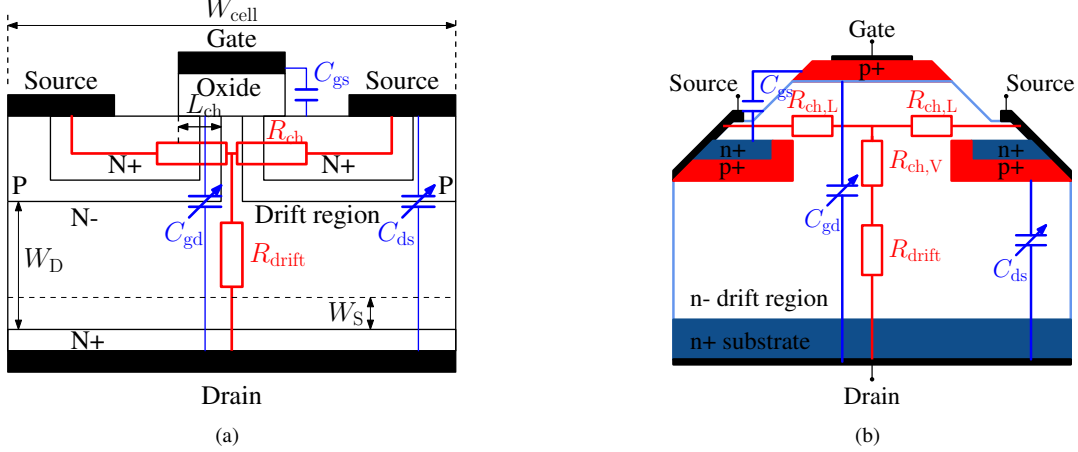


Fig. 1. Structure of different power transistors
(a)MOSFET structure (b)JFET structure

As shown in [10] [11], device specific channel resistance $R_{ch,sp}$ is reversely proportional to channel mobility μ_{ch} and it is almost independent on V_{DSS} voltage, so device $R_{ch,sp}$ does not change when V_{DSS} voltage reduces.

For a 1200V SiC-MOSFET, due to the relatively low electron mobility value of SiC material¹, $R_{ch,sp}$ is about 40% of the total $R_{ON,sp}$ if all the parameters are applied the values given in [12]. Thus, $R_{ON,sp}$ value of a 600V device is about a half that of a 1200V device.

$$\frac{R_{ON,sp,600V}}{R_{ON,sp,1200V}} \approx \frac{1}{2} \quad (3)$$

It is shown in Fig. 1(b) one commercial SiC-JFET structure from Infineon, which is quite similar to MOSFET. There are both lateral and vertical channels inside this JFET, so its $R_{ON,sp}$ are constituted by $R_{drift,sp}$, specific lateral and vertical channel resistances ($R_{ch,L}$ and $R_{ch,V}$). If all the parameters are applied the values givens in [13], $R_{ON,sp}$ of a 600V device is about 60% of a 1200V device. For another type of SiC-JFET (From Siemens) without lateral channel, it is found that $R_{ON,sp}$ of a 600V device is half that of a 1200V device if using all the parameters given in [14].

It can be summarized that when device blocking voltage reduces from 1200V to 600V, device $R_{ON,sp}$ also reduces approximately half.

2.2. Switching loss comparison

Device inter-electrode capacitances C_{gd} , C_{ds} and C_{gs} between each terminal is illustrated in Fig. 1. Unlike C_{gs} , C_{gd} and C_{ds} are V_{DS} voltage dependent capacitances and their values can be approximately calculated by the following equation:

$$C_x = \frac{\epsilon \cdot A_x}{W_S} \quad (4)$$

where C_x refers to either C_{gd} or C_{ds} , A_x refers to each capacitance active area and W_S is depletion region thickness, which is dependent on device switching voltage V_S .

Active area A_x can be obtained by multiplying a device-dependent constant, b , to the device area A . As given in [9], following equation can be used to show the relation between W_D and W_S :

¹electron mobility of SiC varies from 400-900 $\text{cm}^2/\text{V}\cdot\text{s}$ depending on SiC polytypes, which is smaller than Si (around 1300 $\text{cm}^2/\text{V}\cdot\text{s}$).

$$W_S = W_D \cdot \sqrt{\frac{V_S}{V_{DSS}}} \quad (5)$$

By combining above eq.(4) and eq.(5), each capacitor stored charge Q_x during switching is obtained:

$$\begin{aligned} \int_0^{Q_x} dq_x &= \int_0^{V_S} C_x dv_s \\ Q_x &= \frac{2b \cdot \epsilon \cdot A}{W_D} \cdot \sqrt{V_{DSS}} \cdot \sqrt{V_S} \end{aligned} \quad (6)$$

If 600V and 1200V devices switch at the same voltage, their specific charge ($Q_{x,sp}$) comparison can be obtained by following equation:

$$\frac{Q_{x,sp,600V}}{Q_{x,sp,1200V}} = \frac{\sqrt{600}}{\sqrt{1200}} \cdot \frac{W_{D,1200V}}{W_{D,600V}} = 0.7 \cdot \frac{W_{D,1200V}}{W_{D,600V}} \quad (7)$$

By combining eq.(2) and eq.(7) together, it is shown in the following equation that unlike device $R_{ON,sp}$, $Q_{x,sp}$ of 600V device is four times bigger than 1200V device.

$$\frac{Q_{x,sp,600V}}{Q_{x,sp,1200V}} \approx 4 \quad (8)$$

It is shown in Fig. 2 power transistor ideal switching waveforms when device switches at voltage V_S and current I_S . The transistor gate-drain charge Q_{gd} plays an important role in device switching, because its discharge and charge time t by gate current I_g determines switching speed which directly influences device switching losses E_{sw} .

Following equation can be used to approximately calculate device E_{sw} of one switching period by supposing that device has the same turn-ON and turn-OFF switching loss:

$$E_{sw} = V_S \cdot I_S \cdot t = V_S \cdot I_S \cdot \frac{Q_{gd}}{I_g} = V_S \cdot I_S \cdot \frac{Q_{gd}}{V_{com} - V_{pl}} \cdot R_g \quad (9)$$

where V_{com} is controlled gate voltage, V_{pl} is Miller-plateau voltage and R_g is gate resistor.

It is to be noted that device output capacitance C_{oss} (which is the sum of C_{gd} and C_{ds}) stored energy E_{oss} is dissipated in device channel when it is switched ON and E_{oss} is recovered when it is switched OFF. By adding E_{oss} in calculated turn-ON switching loss and subtracting it from calculated turn-OFF switching loss, device total switching loss can still be estimated by eq.(9).

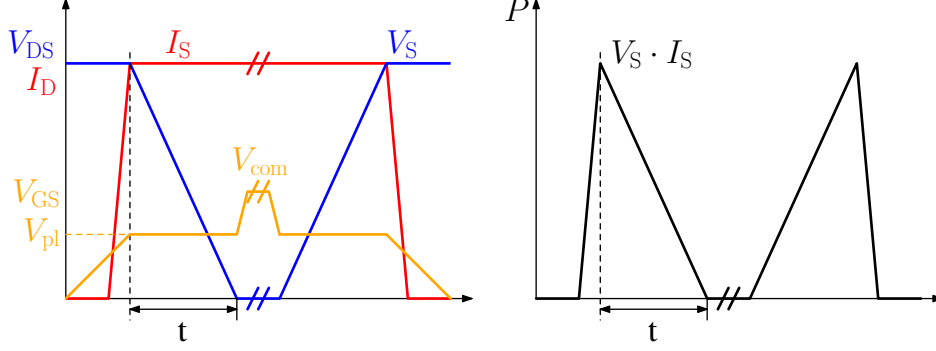


Fig. 2. Ideal switching waveforms and switching losses calculation

Device E_{sw} is shown to be proportional to its Q_{gd} . By normalising for device active area, 600V and 1200V device specific switching loss $E_{sw,sp}$ shall follow the same relation as their specific charge:

$$\frac{E_{sw,sp,600V}}{E_{sw,sp,1200V}} \approx 4 \quad (10)$$

Eq.(10) can be used to compare switching losses between 600V and 1200V devices of the same current rating only when the relative difference in active area is known. This is considered in the following subsection.

2.3. 600V/1200V device comparison

Device conduction current I_D capability is determined by device maximal junction temperature $T_{j(max)}$, which can be obtained by the following equation:

$$I_D^2 \cdot R_{ON} \cdot R_{th} = I_D^2 \cdot \frac{R_{ON,sp}}{A} \cdot R_{th} = T_{j(max)} \quad (11)$$

Initially, only the thermal resistance R_{th} of the die is considered (without device packaging influence), which is given by the following equation showing that it is determined by device thickness (which is assumed to be equal to device drift region thickness W_D), active area A and material thermal conductivity k . Thus,

$$R_{th} = \frac{W_D}{k \cdot A} \quad (12)$$

By combining eq.(11) and eq.(12), I_D can be obtained:

$$I_D = \sqrt{T_{j(max)} \cdot k} \cdot \frac{A}{\sqrt{R_{ON,sp}} \cdot \sqrt{W_D}} \quad (13)$$

If 600V and 1200V devices have the same current rating I_D , k and $T_{j(max)}$, their comparison on device area A is expressed by following equation:

$$\frac{A_{600V}}{A_{1200V}} = \frac{\sqrt{R_{ON,sp,600V}} \cdot \sqrt{W_{D,600V}}}{\sqrt{R_{ON,sp,1200V}} \cdot \sqrt{W_{D,1200V}}} \approx 0.3 \quad (14)$$

By multiplying eq.(14) to eq.(10), 1200V and 600V devices switching losses can then be obtained in the form of the equation below.

$$\frac{E_{sw,600V}}{E_{sw,1200V}} = \frac{E_{sw,sp,600V}}{E_{sw,sp,1200V}} \cdot \frac{A_{600V}}{A_{1200V}} \approx 1.2 \quad (15)$$

In another condition where device packaging influence is considered, device R_{th} is mainly determined by packaging type, where its area and thickness have little contribution on R_{th} value [15]. In this condition, as 600V and 1200V device has the same R_{th} value, their R_{ON} should be identical if their current rating is the same, so A_{600V} is half that of the A_{1200V} . Their switching loss comparison is then shown by the equation below.

$$\frac{E_{sw,600V}}{E_{sw,1200V}} \approx 2 \quad (16)$$

It is found that 600V SiC device switching loss is bigger than 1200V device in both conditions if their current rating is the same.

In the next section, in order to validate the theoretical analysis, SiC and GaN power devices will be experimentally evaluated in order to compare their losses.

3. Experimental validation

3.1. Device characteristics comparison and measurement

ON-state resistance R_{ON} datasheet values of a range of commercial device (listed in Table 1) with similar 30A current rating are compared in Fig. 3(a), which shows that R_{ON} of GaN-HEMT is 25% lower than that of SiC device. R_{ON} of 650V SiC-MOSFET is even 50% higher than 1200V device.

Table 1. Commercial devices using in the experimental validation

	1200V SiC-JFET	1200V SiC-MOSFET	650V SiC-MOSFET	650V GaN-HEMT
Device reference	IJW120R100T1	C2M0080120D	SCT2120AF	GS66508P
Threshold voltage V_{th}	-13.5V	2.6V	2.8V	1.4V

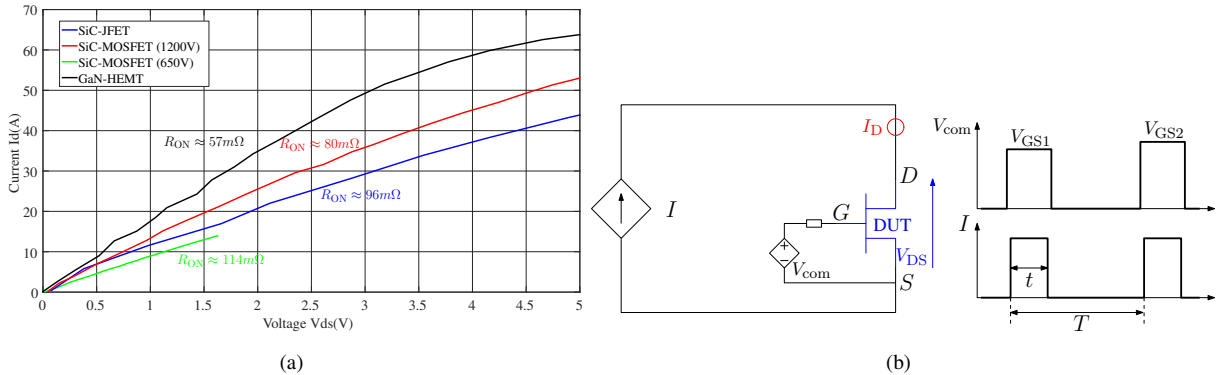


Fig. 3. Device R_{ON} comparison and measurement

(a) Device R_{ON} comparison at 25°C (from datasheet) (b) Electrical circuit to measure R_{ON}

The theoretical study in section 2.1 show that in comparison with a 1200V SiC device with the same current rating, R_{ON} of a 600V SiC is bigger than 1200V device if device active area reduces more than a half (see eq. (3)). Another 600V/40A SiC-MOSFET device [16] (GP1T072A060B, 600V/40A, $V_{th} \approx 2.8V$) shows that its R_{ON} is about 72m Ω , which is still bigger than GaN device of the same current rating.

Device R_{ON} values can be obtained in the experiments either from a curve tracer or from an electrical circuit (shown in Fig. 3(b)), where device voltage V_{DS} and conduction current I_D are measured when they stabilize after applying current pulse I .

Datasheet values of the inter-electrode capacitance comparison of the above devices is shown in Fig. 4. It is found that device input capacitance $C_{iss} = C_{gs} + C_{gd}$ of 650V SiC-MOSFET is slightly bigger than 1200V SiC-MOSFET, and they are bigger than that of GaN-HEMT. Reverse transfer capacitance $C_{rss} = C_{gd}$ of GaN-HEMT is much smaller than that of SiC devices and it is also shown that 650V SiC-MOSFET C_{rss} is bigger than 1200V SiC-MOSFET when bias voltage is beyond 20V. Device output capacitance $C_{oss} = C_{ds} + C_{gd}$ values of the aforementioned devices are similar, among which GaN-HEMT still has the smallest C_{oss} value when V_{DS} is superior to 100V.

If one compares the datasheet of the above 600V/40A SiC-MOSFET with a 1200V/32A SiC-MOSFET [17] (GP1T080A120B, $V_{th} \approx 2.8V$) of another manufacturer (Global Power Technologies Group), it can be noted that inter-electrode capacitances of the former device are also bigger than the latter one.

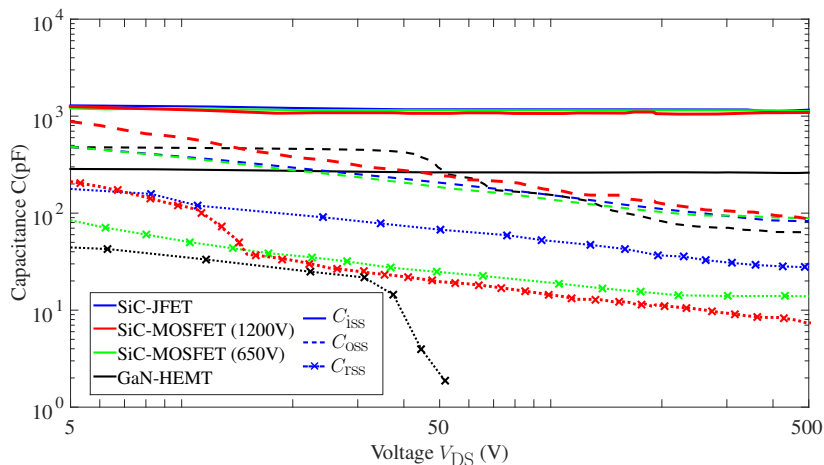


Fig. 4. Inter-electrode capacitance comparison of different SiC and GaN devices

The inter-electrode capacitances values of the GaN-HEMT in Fig. 4 are given on a linear-linear scale in the device datasheet, where it is difficult to extract C_{rss} value due to the strong non-linearity of its value exceeding more than two orders of magnitude. Power semiconductor device inter-electrode capacitances can be measured by small signal method, where device is biased by external DC voltage and small signal can be either generated by an impedance analyzer [18] or by a vector network analyzer [19].

One solution to measure device inter-electrode capacitance is shown in Fig. 5, where an impedance analyzer (IA) and ground connection is used. Device V_{DS} and V_{GS} are biased by external voltage sources. Three external capacitors are used to block the DC voltage between device terminals with IA connector and ground, while their impedance is neglected when passing high frequency (MHz range) AC current. High impedance branches are constituted by three big resistances, which guarantees that all the AC current flow through the transistor. In the electrical circuit shown in Fig. 5,

only current flowing through C_{gd} is measured by IA, because current flowing through capacitance C_{ds} flows to the ground. By varying V_{DS} voltage, device C_{gd} values of different biased voltages are measured. Other measurement circuits can be used to measure C_{gs} and C_{ds} capacitance with similar measurement principle.

By knowing device inter-electrode capacitances, device switching losses can be measured and results will be presented in the next subsection.

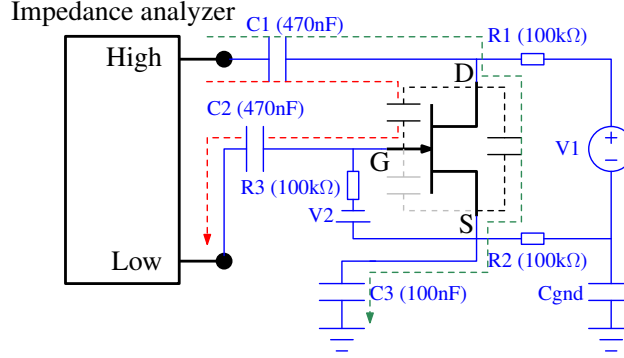


Fig. 5. Power transistor C_{gd} measurement by an impedance analyzer with ground connection

3.2. Device switching losses measurement

3.2.1. Switching circuit: Switching energy E_{sw} of above 1200V/26A SiC-JFET, 650V/29A SiC-MOSFET, 1200V/36A SiC-MOSFET and 650V/30A GaN-HEMT are compared.

The electrical circuit of the switching mesh is shown in Fig. 6(a), in which it is constituted by a bus capacitor C_{bus} , a half bridge circuit with two power semiconductor devices S1 and S2 together with their drivers. Gate mesh and switching mesh of each device is minimized in order to reduce gate mesh inductance $L_{para,g}$ and switching mesh inductance $L_{para,sw}$. Lower device drain switching current I_D and drain source switching voltage V_{DS} are measured to calculate the device switching energy.

The realization switching circuit to test 1200V SiC-JFET is shown in Fig. 6(b), in which the die of the device is mounted in a copper substrate. The device is switched with a gate voltage from -18V to 0V. $L_{para,g}$ can be obtained by measuring gate voltage transient waveform in order to get resonance frequency, which is supposed to be due to resonance between $L_{para,g}$ and device input capacitance C_{iss} . $L_{para,g}$ in the SiC-JFET switching circuit is about 2nH. An AC current probe (P6022, 1kHz-120MHz) is used to measure I_D and an active differential voltage probe (TA043, 100MHz) is used to measure V_{DS} .

The realization switching circuit of 1200V and 650V SiC-MOSFET is shown in Fig. 6(c), where the switching circuit is the same except the packaging type of 1200V device is TO-247 and that of 650V device is TO-220. The same gate voltage from -5V to 20V is used to drive both devices and $L_{para,g}$ in the switching circuit is also about 2nH.

Finally, the realization switching circuit of 650V GaN-HEMT is shown in Fig. 6(d), where device is in GaNPIX package. Gate voltage from 0V to 7V is used to drive the device and measured $L_{para,g}$ in the prototype is around 3nH.

The lumped gate resistance in all the measurements are all around 4Ω, which is composed by gate driver output resistance, external gate mesh resistance and device internal gate resistance. For SiC-MOSFET and GaN-HEMT, devices are driven by the same gate driver IXDN609SI and I_D is

measured by a 1.2GHz current shunt (SSDN-414-025) while V_{DS} is measured by the same differential voltage probe. A high bandwidth oscilloscope up to 1.5GHz is used in the measurement. Switching energy of all the devices are measured by double pulse test in hard switching conditions at room temperature.

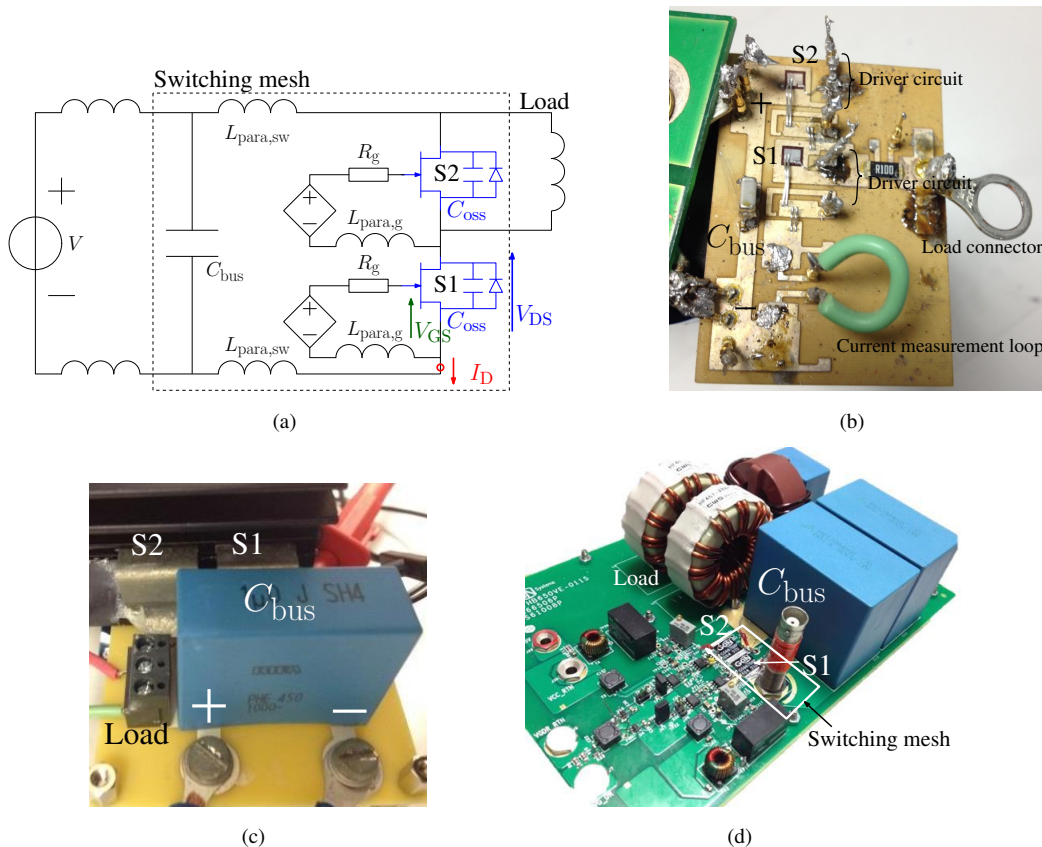


Fig. 6. Electrical circuit of the switching circuit and their realization

(a) Electrical circuit of the switching circuit (b) Switching circuit of SiC-JFET (c) Switching circuit of SiC-MOSFET (d) Switching circuit of GaN-HEMT

3.2.2. Device switching energy comparison in hard switching: The switching waveforms comparison when devices switch at $V_{DS} = 200V$ and $I_D = 5A$ is shown in Fig. 7 while the results when devices switch at $V_{DS} = 300V$ and $I_D = 10A$ is shown in Fig. 8.

The turn-ON transition for GaN-HEMT is indicated from t_1-t_3 in Fig. 7(a) and in Fig. 8(a). During t_1-t_2 , when current I_D starts to rise, the presence of $L_{para,sw}$ induces a voltage drop $L_{para,sw} \cdot \frac{dI_D}{dt}$ of V_{DS} voltage. During t_2-t_3 , V_{DS} voltage decreases to device ON-state voltage $V_{DS(on)}$. Similar turn-ON transition of other devices can be observed in their waveforms.

The turn-OFF transition for GaN-HEMT is indicated from t_6-t_8 in Fig. 7(b) and in Fig. 8(b). During t_6-t_7 , when S1 voltage V_{DS} starts to rise, S2 C_{oss} starts to discharge, which reduces S1 I_D current value, because load current is constant. During t_7-t_8 , S1 I_D starts to decrease to zero, the presence of $L_{para,sw}$ induces a voltage overshoot $L_{para,sw} \cdot \frac{dI_D}{dt}$ of V_{DS} voltage. Similar turn-OFF transition of other devices can be observed in their waveforms.

As shown in the results, when $V_{DS} = 200V$, V_{DS} turn-OFF transition time (from 10% to 90% switching voltage) of 1200V SiC-MOSFET is around 12ns while that of 650V SiC-MOSFET is

around 15ns. When $V_{DS} = 300V$, V_{DS} turn-OFF transition time of 1200V SiC-MOSFET is around 15ns while that of 650V SiC-MOSFET is around 16ns, indicating that 1200V SiC-MOSFET switches faster than 650V SiC-MOSFET in turn-OFF switching, which is supposed to be because the transfer capacitance C_{rss} of 1200V device is smaller than 650V device in high voltage.

In terms of turn-ON switching, when $I_D = 5A$ and $I_D = 10A$, current transition time (from 10% to 90% peak current) for both 1200V and 650V SiC-MOSFET is quite similar, which is around 7ns and 8ns separately, suggesting a similar device input capacitance C_{iss} , which corresponds with their C_{iss} datasheet value (C_{iss} of 1200V device is slightly smaller than 650V device).

When comparing with 650V GaN-HEMT, it is shown that GaN-HEMT current turn-ON transition time is around 5ns in both switching conditions, which confirms the datasheet value that C_{iss} of GaN-HEMT is only about one sixth of 1200V SiC-MOSFET. In terms of turn-OFF switching, when $V_{DS} = 200V$ and $V_{DS} = 300V$, GaN-HEMT voltage transition time is around 8ns and 6ns separately, confirming its smaller C_{rss} value than SiC devices.

When comparing SiC-JFET with GaN-HEMT, it is observed that both V_{DS} and I_D transition time of GaN-HEMT is shorter than SiC-JFET in the above switching conditions, which also confirms that GaN-HEMT has smaller inter-electrode capacitances than SiC-JFET.

It can be thus concluded that GaN-HEMT switches faster than SiC power transistors and 1200V SiC-MOSFET switches faster than 650V SiC-MOSFET.

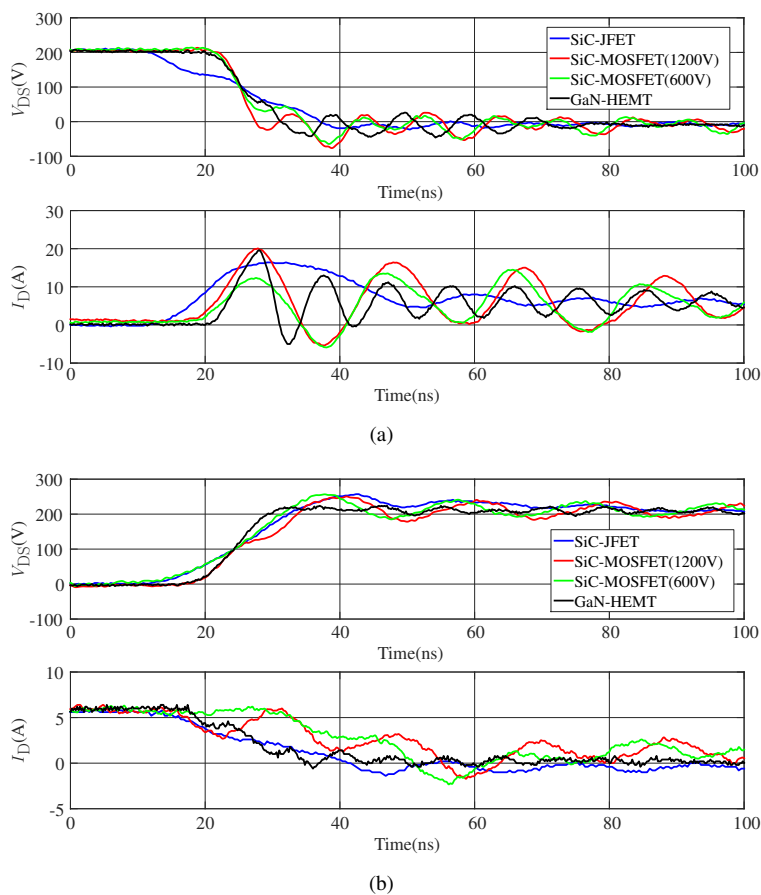


Fig. 7. Switching waveforms comparison when device switches at $V_{DS} = 200V$ and $I_D = 5A$
(a) Device ON (b) Device OFF

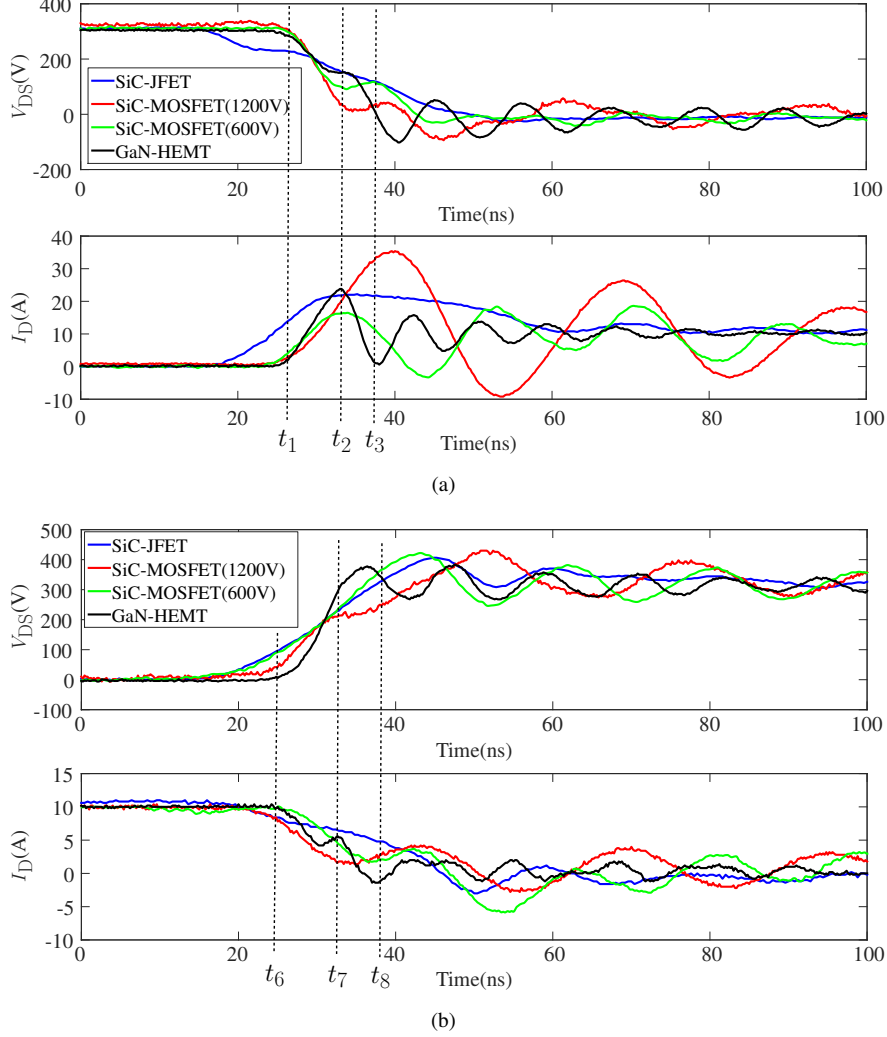


Fig. 8. Switching waveforms comparison when device switches at $V_{DS} = 300V$ and $I_D = 10A$
(a) Device ON (b) Device OFF

It is shown in Fig. 9 the switching energy E_{sw} comparison results of all the aforementioned devices when they switch at both 200V and 300V. It is to be noted that device C_{oss} discharge current is excluded in the measured I_D current when device is switched ON, so device C_{oss} stored energy E_{oss} is dissipated and it is excluded in obtained turn-ON switching energy. In contrary, C_{oss} charge current is included in I_D current when device is switched OFF, so E_{oss} is included in obtained turn-OFF switching energy.

It is shown in those results that E_{sw} of 1200V SiC-MOSFET is smaller than that of 650V SiC-MOSFET, which confirms the theoretical analysis. When comparing with SiC device, E_{sw} of GaN-HEMT is even smaller, which shows that it is more suitable for below 300V electrical energy conversion than SiC devices.

It is also shown that obtained GaN-HEMT turn-ON E_{sw} is very close to SiC-MOSFET at some switching conditions. This is supposed to be the difference of $L_{para,sw}$ in device switching mesh, which is due to the difference of device packaging type. $L_{para,sw}$ value in SiC-MOSFET switching mesh is measured to be 80nH, which is bigger than measured 36nH in GaN-HEMT switching mesh. Bigger $L_{para,sw}$ value causes bigger voltage drop across it when I_D is rising at turn-ON

switching, which decreases overlapping time between switching voltage and current. This snubber effect results in a small measured turn-ON switching energy value in SiC-MOSFET switching circuit.

For both GaN-HEMT and 1200V SiC-MOSFET, device turn-ON E_{sw} are larger than turn-OFF E_{sw} and therefore those devices will benefit from zero voltage switching (ZVS) where turn-ON losses can be eliminated. Further switching measurements for these devices under ZVS condition will be presented in the following section. In power electronics systems, normally-OFF devices are more preferable than normally-ON devices because of safe reason in case of gate driver fault, so normally-ON SiC-JFET is not considered in the following analysis.

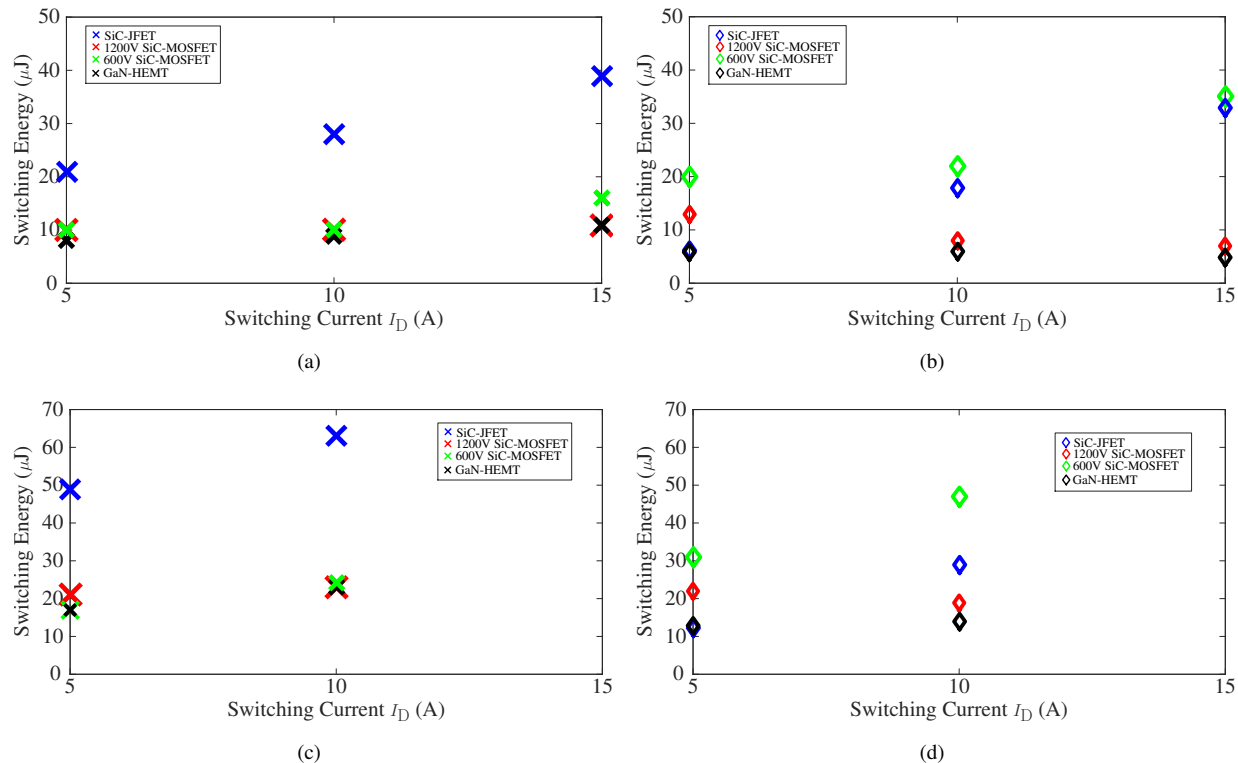


Fig. 9. Device switching energy comparison of different switching conditions

(a) Turn-ON E_{sw} ($V_{DS} = 200V$) (b) Turn-OFF E_{sw} ($V_{DS} = 200V$) (c) Turn-ON E_{sw} ($V_{DS} = 300V$) (d) Turn-OFF E_{sw} ($V_{DS} = 300V$)

3.2.3. Device switching energy comparison in soft switching: It is illustrated in Fig. 10(a) device soft switching circuit. Unlike device hard switching circuit, another external power supply is used to maintain output capacitor C_{out} voltage constant. Devices S1 and S2 area controlled by the signal shown in Fig. 10(b).

At instant t_1 , device S2 is switched ON and device S1 remains OFF, so output inductor L is started to be charged by input and output voltage difference $V_{in} - V_{out}$. Afterwards at instant t_2 , S2 is switched OFF, so its C_{oss} is charged by one part of the output inductor current I_L . Meanwhile, voltage across S1 drops when voltage across S2 increases, so S1 C_{oss} is discharged by one part of I_L , and its stored energy E_{oss} is transferred to the device S2. After deadtime dt , which is supposed to be longer than S1 and S2 E_{oss} transfer time, device S1 is switched ON. At this switching cycle, S2 switches OFF in hard switching mode at t_2 and S1 switches ON in ZVS soft switching mode.

Then, L is reversely charged by output voltage V_{out} , so I_L changes the direction. At instant t_3 , S1 is switched OFF in hard switching mode and like previous switching cycle, stored energy in C_{oss} of S2 is transferred by one part of I_L to C_{oss} of S1. After deadtime, S2 is switched ON at ZVS soft switching mode and finally at instant t_4 , it is switched OFF at hard switching condition.

Based on the above control signals, I_L current waveform is illustrated in Fig. 10(b). For device S1, it only has turn-OFF switching loss at instant t_3 which is due to the overlapping of V_{DS} and I_D . It does not have any more turn-ON switching loss at instant t_2+dt . Similar as S1, S2 only has turn-OFF switching loss at instant t_2 and t_4 and it does not have any more turn-ON switching loss at instant t_3+dt . S1 E_{oss} is transferred to S2 before switching ON and vice versa, so device total switching losses is reduced in this switching circuit.

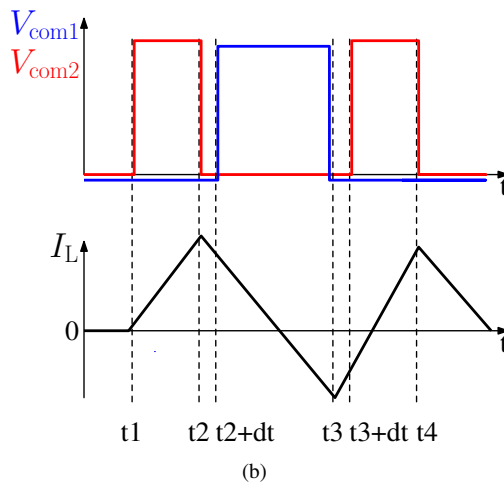
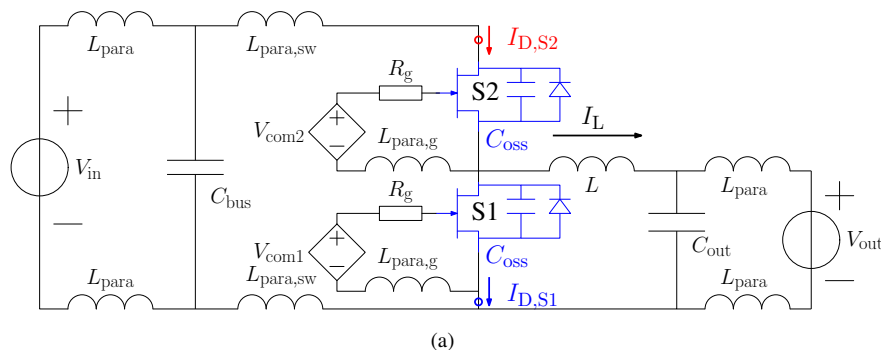


Fig. 10. Electrical circuit using to test device in soft switching and load current waveform
(a) Electrical circuit (b) Control signals with load current waveform

It is shown in Fig. 11(a) measured load current I_L waveform and in Fig. 11(b) measured switching waveforms of 1200V SiC-MOSFET S1, S2 in this switching circuit when $V_{in} = 300V$ and $V_{out} = 50V$. As analysed previously, at instant t , device S2 is switched OFF in hard switching mode and E_{oss} of device S1 is transferred to S2, where a zoomed figure to illustrate S1 turn-ON at soft switching mode is shown in Fig. 11(c). By multiplying measured transient current and voltage waveforms, switching power waveforms of each device are obtained and they are shown in Fig. 11(d). Thus, S2 turn-OFF energy including E_{oss} and S1 E_{oss} can be obtained separately. As S1 and S2 are identical devices, its turn-OFF switching loss due to switching current and voltage overlapping can be obtained by subtracting E_{oss} . Based on the obtained waveform, when 1200V

SiC-MOSFET is switching at 300V, its E_{OSS} is about $4.4\mu\text{J}$.

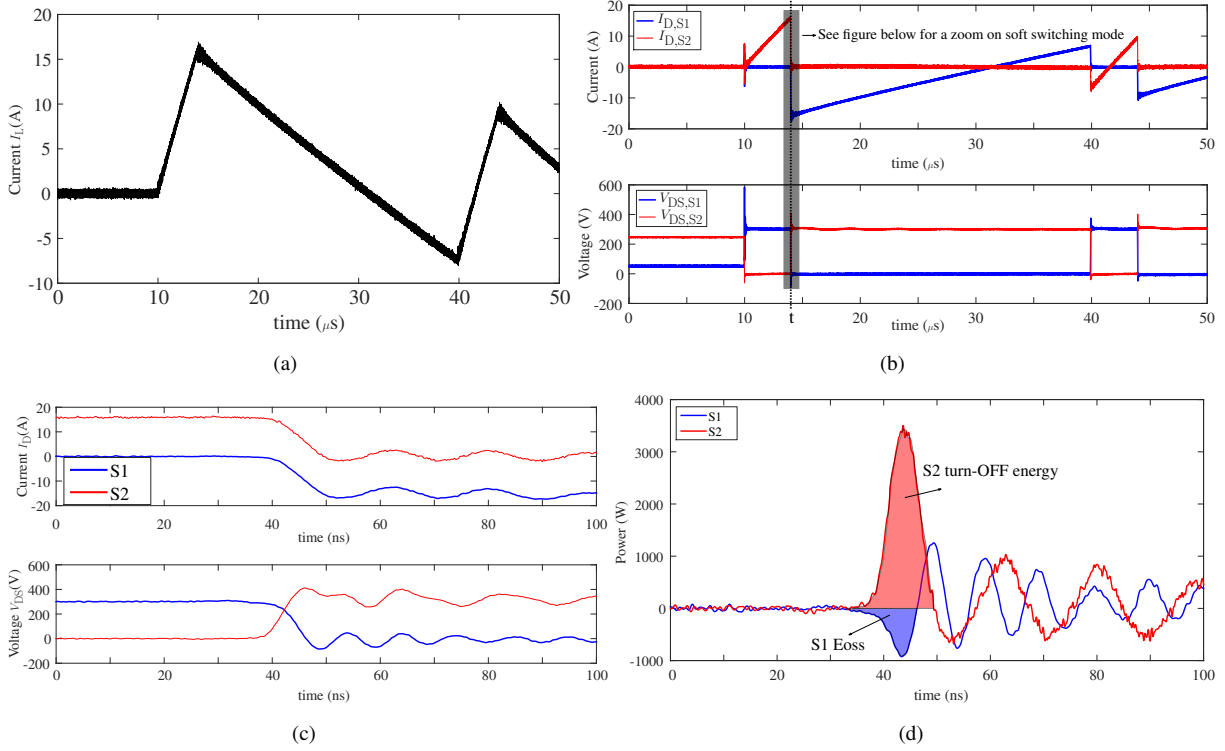


Fig. 11. Measured 1200V SiC-MOSFET switching waveforms and E_{OSS} when it switches at 300V/15A in soft switching

(a) Load current waveform (b) Device switching waveforms (c) Zoomed device switching waveforms on soft switching mode (d) Device turn-OFF energy and E_{OSS}

It is compared in Fig. 12 measured E_{OSS} of all the aforementioned devices, which shows that E_{OSS} of all the devices is close to each other. The GaN-HEMT is evaluated at 300V in soft switching mode, which shows more experimental results than original results presented by authors in [8]. This result confirms with device C_{OSS} values given in Fig. 4. By subtracting E_{OSS} from device turn-OFF energy given in Fig. 9, device switching losses in this switching mode is compared in Fig. 13, where it is shown that 1200V SiC-MOSFET still has less switching losses than 650V SiC-MOSFET and GaN device has less switching losses than SiC device in ZVS soft switching mode.

By combining all the above measurement results, it is shown that GaN device produces less switching loss in comparison with a 600V or 1200V SiC device with the same current rating and it is more suitable than SiC device to be applied in below 300V energy conversion.

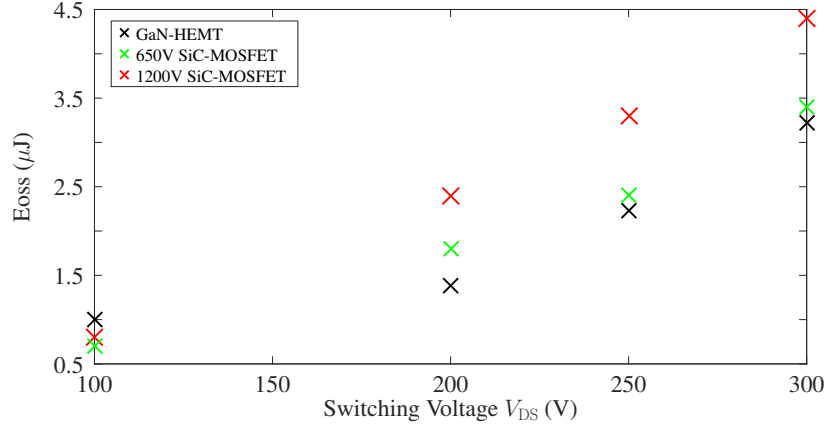


Fig. 12. Device stored energy E_{oss} comparison of different SiC and GaN devices

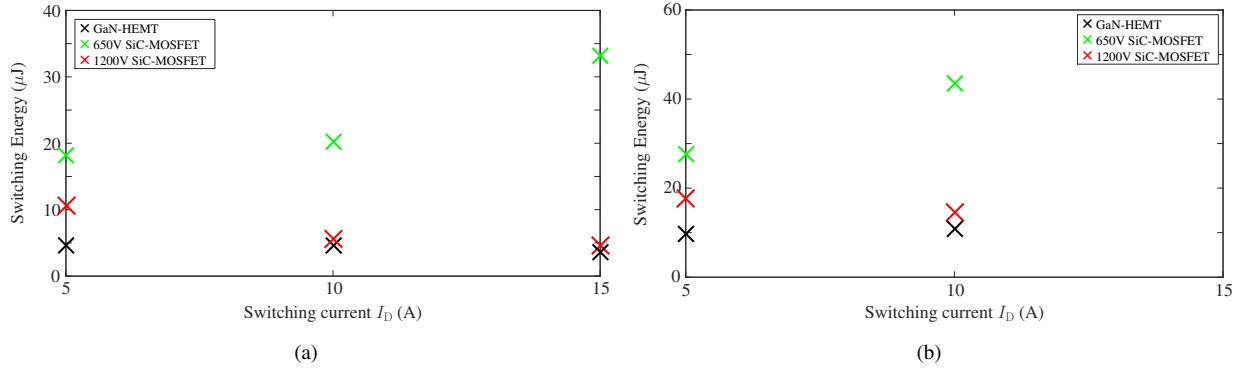


Fig. 13. Device switching losses comparison under ZVS soft switching mode
(a) $V_{DS} = 200V$ (b) $V_{DS} = 300V$

4. Conclusion

Conduction loss and switching loss of SiC and GaN power semiconductor devices are compared in the paper. In order to compare losses of devices with the same power rating, a theoretical analysis is given, where it is shown that SiC power transistors specific ON-state resistance ($m\Omega \cdot mm^2$) will reduce half if device maximal blocking voltage decreases from 1200V to 600V. Unlike device specific ON-state resistance, device specific capacitance value (F/mm^2) of 600V device is four times bigger than 1200V device. Due to SiC material low mobility, it is thus found that ON-state resistance $R_{ON}(m\Omega)$ and inter-electrode capacitance (F) of 1200V SiC device is smaller than 600V SiC device if two devices have the same current rating, suggesting a lower conduction loss and switching loss of 1200V SiC device.

In order to validate the theoretical analysis, static and dynamic characteristics of 1200V and 600V SiC power transistors are at first compared with 600V GaN-HEMT, in which it is shown that GaN-HEMT has smaller R_{ON} and inter-electrode capacitances than SiC devices. Meanwhile, R_{ON} and inter-electrode capacitances values of a 600V SiC-MOSFET is even bigger than a 1200V device in some voltage range.

Afterwards, switching energy E_{sw} of those devices are compared in hard switching mode, where

it is shown that GaN-HEMT has less E_{sw} than all the SiC transistors (JFET, MOSFET) and 1200V SiC-MOSFET has less E_{sw} than 650V SiC-MOSFET, which confirms the theoretical analysis. It is also shown in the results that 1200V SiC-MOSFET and 650V GaN-HEMT have bigger turn-ON E_{sw} than turn-OFF E_{sw} .

In order to reduce device turn-ON E_{sw} , a zero voltage switching (ZVS) circuit is used to evaluate devices in soft switching mode. Device output capacitance stored energy E_{oss} can thus be measured, so device turn-OFF losses due to switching current and voltage overlapping can be obtained. By subtracting E_{oss} , it is shown that GaN-HEMT has less switching losses than SiC devices in ZVS soft switching mode and 1200V SiC-MOSFET still has less switching losses than 600V SiC-MOSFET.

Based on all the experimental results, it can be concluded that 1200V SiC-MOSFET has less switching losses than 600V SiC-MOSFET in both hard and soft switching mode and GaN-HEMT is more suitable than SiC devices for vehicle based power electronics systems in below 300V electrical energy conversion.

5. Acknowledgment

The work was funded by the UK Engineering and Physical Sciences Research Council (EPSRC) through research grant [EP/K014471/1]. The authors would like to thank all the partners of the project Silicon Compatible GaN Power Electronics for technical discussions.

6. References

- [1] Allegre, A. L., Bouscayrol, A., and Trigui, R.: 'Flexible real-time control of a hybrid energy storage system for electric vehicles', IET Electrical Systems in Transportation, 2013, 3, (3), pp. 79–85
- [2] Wang, J.: 'Practical design considerations of power electronics in hybrid and fuel cell vehicles'. Proc. 2008 IEEE Vehicle Power and Propulsion Conference, Sept 2008, pp. 1–6
- [3] Schlting, P., Rosekeit, M., Garikoitz, S., Biskoping, M., and Doncker, R. D.: 'Potential of using gan devices within air cooled bidirectional battery chargers for electric vehicles.' Proc. 2015 IEEE 6th International Symposium on Power Electronics for Distributed Generation Systems (PEDG), June 2015, pp. 1–6
- [4] Srdic, S., Zhang, C., Liang, X., Yu, W., and Lukic, S.: 'A SiC-based power converter module for medium-voltage fast charger for plug-in electric vehicles'. Proc. 2016 IEEE Applied Power Electronics Conference and Exposition (APEC), March 2016, pp. 2714–2719
- [5] Chinthavali, M., Otaduy, P., and Ozpineci, B.: 'Comparison of Si and SiC inverters for IPM traction drive'. Proc. 2010 IEEE Energy Conversion Congress and Exposition, Sept 2010, pp. 3360–3365
- [6] Acanski, M., Popovic-Gerber, J., and Ferreira, J. A.: 'Comparison of Si and GaN power devices used in PV module integrated converters'. Proc. 2011 IEEE Energy Conversion Congress and Exposition, Sept 2011, pp. 1217–1223

- [7] Li, K., Evans, P., and Johnson, M.: 'SiC/GaN Power Semiconductor Devices Theoretical Comparison and Experimental Evaluation'. Proc. 2016 IEEE Vehicle Power and Propulsion Conference (VPPC), Oct 2016, pp. 1–6
- [8] Li, K., Evans, P., and Johnson, M.: 'SiC and GaN power transistors switching energy evaluation in hard and soft switching conditions'. Proc. 2016 IEEE 4th Workshop on Wide Bandgap Power Devices and Applications (WiPDA), Nov 2016, pp. 123–128
- [9] Lutz, J., Schlangenotto, H., Scheuermann, U., and De Doncker, R.: 'Semiconductor Power Devices'. Springer, 2011
- [10] Baliga, B.: 'Advanced High Voltage Power Device Concepts'. Springer, 2011
- [11] Ueda, D., Takagi, H., and Kano, G.: 'A new vertical power MOSFET structure with extremely reduced on-resistance', IEEE Transactions on Electron Devices, 1985, 32, (1), pp. 2–6
- [12] Ruff, M., Mitlehner, H., and Helbig, R.: 'SiC devices: physics and numerical simulation', IEEE Transactions on Electron Devices, 1994, 41, (6), pp. 1040–1054
- [13] Mousa, R.: 'Caractrisation, modlisation et intgration de JFET de puissance en carbure de silicium dans des convertisseurs haute temprature et haute tension'. PhD thesis, L'INSA de Lyon, 2009.
- [14] Friedrichs, P., Mitlehner, H., Dohnke, K.O., Peters, D. et al.: 'SiC power devices with low on-resistance for fast switching applications'. Proc. The 12th International Symposium on Power Semiconductor Devices and ICs, 2000, pp. 213–216
- [15] Wu, H., Chen, M., Gao, L., and Li, M.: 'Thermal resistance analysis by numerical method for power device packaging', Proc. 2012 13th International Conference on Electronic Packaging Technology and High Density Packaging (ICEPT-HDP), Aug 2012, pp. 666–670
- [16] Global Power Technologies Group: 'GP1T072A060B datasheet', 2016.
- [17] Global Power Technologies Group: 'GP1T080A120B datasheet', 2016.
- [18] Chen, Z., Boroyevich, D., Burgos, R., and Wang, F.: 'Characterization and modeling of 1.2 kV, 20A SiC MOSFETs', Proc. 2009 IEEE Energy Conversion Congress and Exposition, Sept. 2009, pp. 1480–1487
- [19] Li, K., Videt, A., and Idir, N.: 'Multiprobe Measurement Method for Voltage-Dependent Capacitances of Power Semiconductor Devices in High Voltage', IEEE Transactions on Power Electronics, 2013, 28, (11), pp. 5414–5422